

# Out-of-phase mixed-mode oscillations of two strongly coupled identical relaxation oscillators

Maksim N. Stolyarov, Victor A. Romanov, and Evgenii I. Volkov

*Department of Theoretical Physics, P. N. Lebedev Physical Institute, Leninskii 53, 117924 Moscow, Russia*

(Received 17 October 1995)

We analyzed bifurcations of periodic regimes generated in the systems of two identical relaxation oscillators under strong coupling through a “slow” (inhibitory) variable. It was numerically shown that complex spatiotemporal behavior is observed near the boundaries of stability of the known antiphase periodic attractor and inhomogeneous steady states. Specifically, the following attractors were found: (i) a set of cycles of the antiphase type, each of which consists of one full-amplitude excursion and of the different number of small-amplitude high-frequency oscillations (the period of antiphase mixed-mode regimes is much greater than that of simple antiphase oscillations), (ii) inhomogeneous regimes of the above described type (out-of-phase mixed mode) with unequal numbers of small oscillations for different oscillators, (iii) period doubling cascades of the out-of-phase mixed mode that lead to the appearance of chaotic attractors. We showed that the modes found are not specific for our particular model; however, they are common for several classes of models and sensitive to the stiffness of oscillators. We discuss also conditions for the generation of such regimes. [S1063-651X(96)06806-7]

PACS number(s): 05.45.+b, 47.20.Ky, 82.40.Bj

## I. INTRODUCTION

In coupled oscillatory systems, the primary interest was directed to the question of how local oscillators are entrained to common collective oscillations. The studies of coupled oscillatory units are useful for the understanding of spatiotemporal patterning in electronics [1,2], physiology [3], chemistry [4,5], etc. Relaxation oscillators represent an important class of nonlinear systems describing many natural and artificial phenomena characterized by very different time scales [6–10].

Since the work of Lefever and Prigogine [11] the behavior of two coupled oscillators was a subject of extensive investigations. It was shown that the simplest diffusive coupling of identical oscillators can provide the existence of the antiphase limit cycle that is realized in many models [6,12–15]. The antiphase limit cycle may be considered as the universal model-independent attractor [14,16–18]. In this mode, the wave forms of both oscillators are identical except for a half-period shift. In addition to periodic modes, stable stationary states emerge because oscillators may stop each other due to coupling. The chemical [6,12] and electronic [19] experiments confirmed the existence of the 180° out-of-phase regime and inhomogeneous steady states [20] and showed a general character of these modes and their insensitivity to noise and other experimental details, including weak nonidenticality.

Bistability of the in-phase and antiphase limit cycles was studied in the framework of membrane model of cell cycle regulation [21]. It was shown that the bistability of the two periodic regimes in the phase diagram is a typical phenomenon and the stiffer the oscillators, the larger the volume of parameter space involved in the bistability region. The coexistence of several periodic solutions was investigated in detail for two Brusselators taken not far from the Hopf bifurcation [22]. In this area of parameters, the wave forms are smooth enough and the phase diagram is very rich.

In this paper, we concentrate on *stiff* oscillators coupled

through their slow variables and find unusual regimes of the out-of-phase type that are realized in the range of strong interactions (near the stable inhomogeneous steady-state region). These regimes look like they are “bursting” and are characterized by the existence of small-amplitude high-frequency oscillations that alternate with the single large-amplitude long-period cycle. In the partial phase plane ( $X_i, Y_i$ ) they appear as small loops on the partial “limit cycle” (more exactly, on the projection of the four-dimensional limit cycle in the partial phase plane). Following [23], we will call these regimes mixed mode. However, the similarity of the mixing mechanisms described for three-variable oscillators [23,24] and for the coupled two-variable oscillators should be considered separately.

Despite seeming temporal complexity, the mixed-mode regime is symmetrical with respect to a half-period shift. A detailed continuation of this regime in parameters permits a break of the symmetry to be revealed. A break of the symmetry gives rise to the spatially inhomogeneous limit cycles (out-of-phase mixed mode) that have the loops on different parts of trajectories of the two oscillators.

## II. MODELS

### A. Membrane oscillator

The membrane model is a result of the reduction of many equations describing the process of lipid peroxidation in biological membranes [25], and may be simplified and written in the dimensionless form

$$\frac{dX}{dt} = \frac{1}{\varepsilon} \left\{ \kappa + \frac{1}{2}XY - X^2 - \frac{3}{2} \frac{\gamma X}{X + \delta} \right\}, \quad (1a)$$

$$\frac{dY}{dt} = \eta - \kappa - \frac{3}{2}XY - DY - \frac{1}{2} \frac{\gamma X}{X + \delta}. \quad (1b)$$

The parameter  $\varepsilon$  specifies the time scale and is varied between 0.1 and 0.001. Here  $X, Y$  are dimensionless concen-

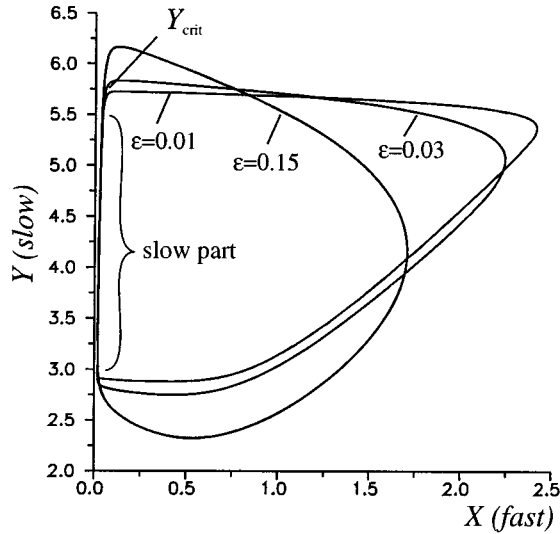


FIG. 1. The phase portrait of system (1) for  $\gamma=0.5$ ,  $\delta=0.15$ ,  $\kappa=0.05$ ,  $D=0.2$  fixed throughout this paper.  $\eta=2.56$ . Other designations are explained in the text.

trations of radicals (“fast” variable) and lipids (“slow” variable), respectively.  $\kappa$ ,  $\gamma$ ,  $\delta$ ,  $D$ ,  $\eta$  are the rates of influx and efflux of participants. The first four rates are fixed hereafter and only  $\eta$  will be considered as a bifurcation parameter for different  $\varepsilon$ .

Let us summarize essential features of the oscillator:

(i) The form of the limit cycle and consequently the amplitudes of variables are remarkably insensitive to changes in the bifurcation parameter  $\eta$  at least up to  $\eta=2.8$  because  $\eta$  does not enter Eq. (1a) for the  $N$ -shaped nullcline. The phase portrait of the membrane oscillator for different  $\varepsilon$  and the time series  $X(t)$  and  $Y(t)$  are presented in Figs. 1 and 2,

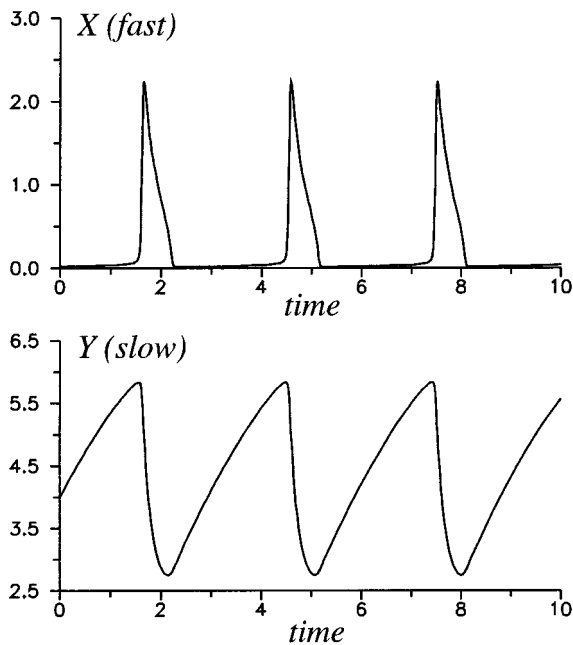


FIG. 2. The time series of (1) for “fast,”  $X(t)$ , and “slow,”  $Y(t)$ , variables for  $\eta=2.56$ ,  $\varepsilon=0.03$ .

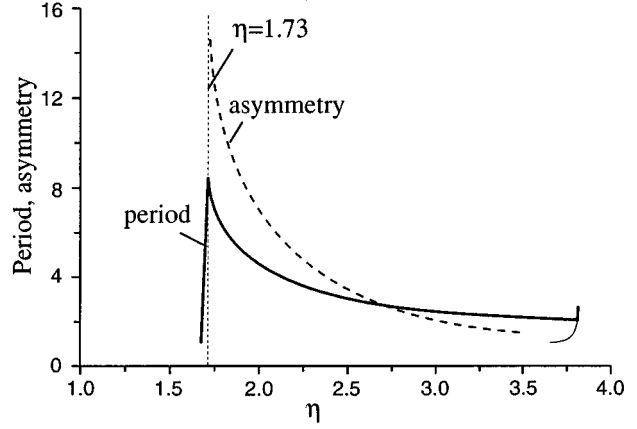


FIG. 3. Period and asymmetry of individual oscillations as a function of  $\eta$  for  $\varepsilon=0.01$ . The Hopf bifurcation with the canard transition occurs at  $\eta \approx 1.73$ .

respectively.

(ii) The period strongly depends on the value of the bifurcation parameter  $\eta$  as it is shown in Fig. 3. Such a dependence of the period on the control parameter is typical of the Hopf bifurcation with the canard transition [21], which happens at  $\eta \approx 1.73$ . The period has a *finite* maximum value. The nearly vertical solid line corresponds to a very narrow region where Hopf’s limit cycle develops into a large amplitude limit cycle. As  $\eta$  increases, the cycle disappears via *subcritical* the Hopf bifurcation at  $\eta \approx 3.85$ . This bifurcation assumes (see Fig. 3) that two attractors (the stable focus and stable limit cycle) coexist in a region around the bifurcation point. The width of the bistability region strongly depends on the value of the relaxation parameter  $\varepsilon$ : the greater the stiffness, the narrower the region.

(iii) The form of oscillations  $X(t)$ ,  $Y(t)$  for  $\varepsilon < 0.05$  is highly asymmetrical (Fig. 2), i. e., the times spent on left ( $T_{left}$ ) and right ( $T_{right}$ ) branches of the  $N$ -shaped nullcline  $dX/dt=0$  are very different:  $T_{left} \gg T_{right} \gg T_{jump}$ , where  $T_{jump}$  is the time of jumps between the nullcline branches. The degree of asymmetry will be characterized by the ratio  $\alpha = T_{left}/T_{right}$ , which grows as the system approaches the singular bifurcation at  $\eta \approx 1.73$  (Fig. 3). This occurs because the phase rate of a representative point in the vicinity of  $Y_{crit}$  (see Fig. 1) tends to zero but the form of the cycle remains unchanged (except for a very narrow region of the Hopf bifurcation with the canard transition). The degree of asymmetry of the oscillator is essential for generating inhomogeneous regimes in the system of coupled oscillators (see [21]).

## B. The Brusselator

In order to check the generality of results obtained, we use the popular Brusselator, which is a typical model of the so-called  $\lambda$ -oscillators with classical supercritical Hopf’s bifurcation of the cycle birth. The well known equations for the Brusselator are presented here for the sake of convenience:

$$\frac{dX}{dt} = A - (B+1)X + X^2Y, \quad (2a)$$

$$\frac{dY}{dt} = BX - X^2Y. \quad (2b)$$

We chose  $A=2$  and  $B$  large enough in order to ensure that the Brusselator was a relaxation oscillator in which  $Y$  is a slow variable. The steady state of the system  $X_s=A$ ,  $Y_s=B/A$  loses stability if  $B=A^2+1$  at *supercritical* Hopf bifurcation, and a stable limit cycle appears. In contrast to the membrane oscillator, the Brusselator has a trianglelike phase portrait. The size of the limit cycle and the period of the oscillations are proportional to  $(B+1)^2$ .

We will consider two identical oscillators coupled symmetrically but through a semipermeable membrane. It means that the diffusive term  $C(Y_{i+1}-Y_i)$ ,  $i=1, 2$  is added only to the second equation of each oscillator:

$$\begin{aligned} \frac{dX_i}{dt} &= F(X_i, Y_i), \\ \frac{dY_i}{dt} &= G(X_i, Y_i) + C(Y_{i+1} - Y_i), \end{aligned} \quad (3)$$

$$i=1, 2.$$

The coupling we use is not the most general because we disregard coupling through the fast variables, but such a simplification is justified for relaxation systems in which inhomogeneous regimes may be destroyed by coupling through the fast variable exchange affecting the most sensitive slow part of the cycles (see also [17,18]).

It should be noted that, for two membrane oscillators, the form and the amplitude of the cycle remain almost unchanged when we vary the stiffness ( $\varepsilon$ ), asymmetry (as a function of  $\eta$ ), and diffusive coupling strength ( $C$ ), whereas any variation of  $A, B, C$  in the system of two coupled Brusselators significantly affects the form and the amplitude of the cycle and thereby changes the diffusion flow between Brusselators. In particular, comparing the results for very different values of  $B$ , it would be reasonable to rescale the values of  $C$  in order to provide the same intensity of diffusion.

### III. METHODS

All the results presented below are based upon numerical computations. We used an explicit fourth order (double precision) Runge-Kutta routine with step size control (subroutine named DRKGS from the old scientific library SSP), which is a good and reliable method for equations that are not very stiff. Checking the existence of spurious solutions (when we had some doubts) was performed using the package AUTO [26]. AUTO was used in both parametrical analysis of steady states and investigation of periodic solutions near their bifurcations. Special attention was paid to the analysis of transient regimes. We examined periodic solutions obtained with DRKGS and implicit integrators (RADAU5 was found to be very useful) and found no difference between them within the limits of the computational errors.

It was a problem to search for solutions for the desirable values of the parameters. We adopted the following simple strategy: starting from a random initial point, we solved the

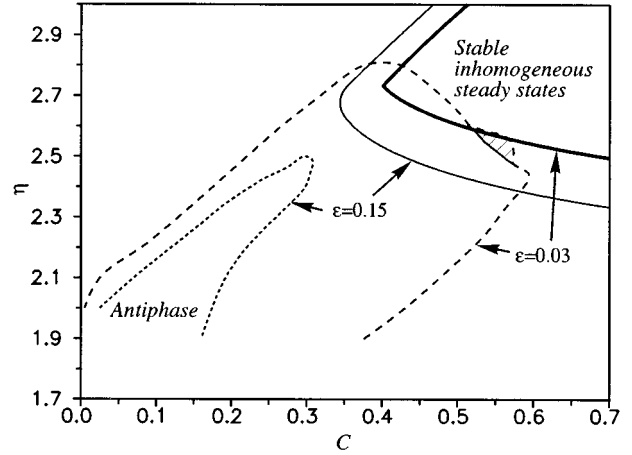


FIG. 4. The phase diagram of (1) on the  $(C, \eta)$  plane for  $\varepsilon=0.15, 0.03$ . The regions of antiphase oscillations are outlined by the dashed lines. The shadowed region corresponds to the localization of mixed-mode cycles. Solid lines are boundaries of the region of the inhomogeneous steady states.

chosen equations until an asymptotic behavior (“attractor”) was obtained with the needed accuracy. This attractor was classified. The procedure was repeated for another initial point. The strategy found different types of coexisting attractors for the chosen set of parameters. We then changed the parameters and repeated the whole procedure.

## IV. RESULTS

### A. Overview of basic solutions

The large-scale phase diagrams of the system of coupled membrane oscillators in the  $(C, \eta)$ -parameter plane for  $\varepsilon=0.15, 0.03$  are shown in Fig. 4. The antiphase stable periodic solution (the wave form is presented in Fig. 5) occupies an essential part of the control parameter plane  $(C, \eta)$ . The regime coexists with the in-phase solution, which is stable everywhere over the presented phase diagram. We also found that, for strong coupling, bistability between the antiphase mode and inhomogeneous steady states is possible but only if the stiffness of the coupled oscillators is greater than a certain critical value. For the membrane oscillator it means that  $\varepsilon < 0.12$  or  $A > 1.23$  for Brusselator. The coexistence of three stable attractors (the in-phase and antiphase regimes and inhomogeneous steady states) occurs (see Fig. 4 for  $\varepsilon=0.03$ ) without an infinite period bifurcation, which is typically expected [6] in such a situation. To study the new relations between the antiphase regime and inhomogeneous steady states the evolution of the antiphase limit cycle should be investigated in the vicinity of the overlapping area.

### B. Two kinds of antiphase solutions

The parameter continuation performed using AUTO shows that the stable antiphase solution ends in the pitchfork bifurcation BP (Fig. 6) or fold type catastrophe (dangerous bifurcation in terms [27] because the system abruptly changes its behavior). The ordinate gives the norm of the solutions, which is defined as

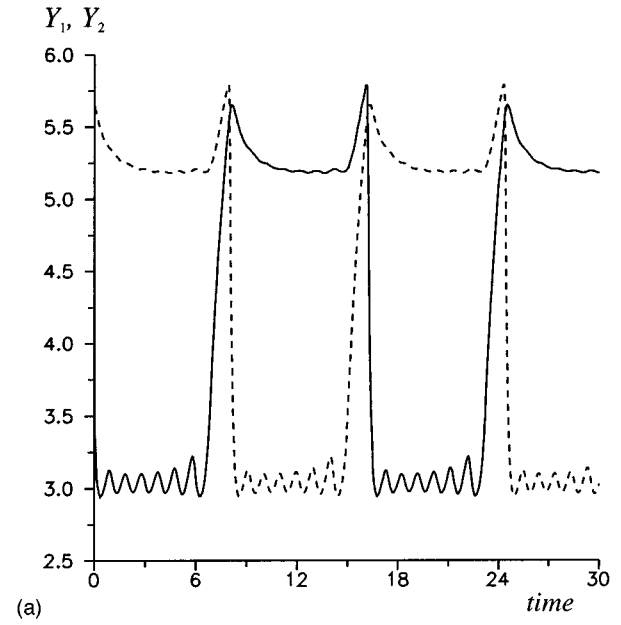
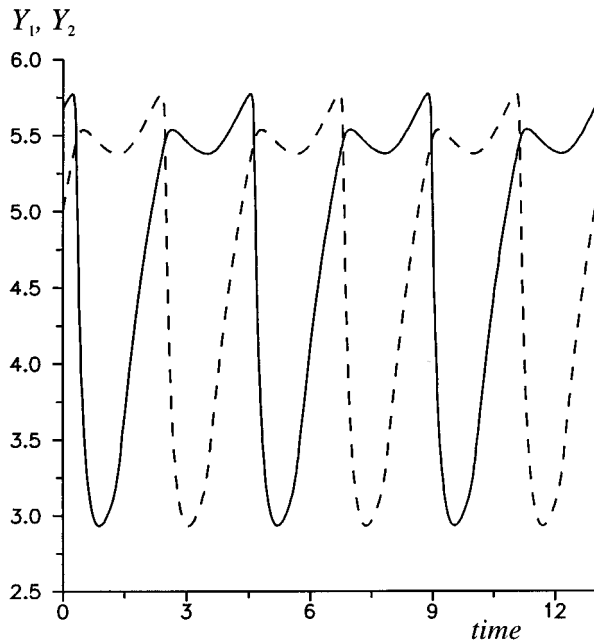


FIG. 5. The wave forms of the slow variables  $Y_1, Y_2$  for the antiphase limit cycle,  $\eta=2.56$ ,  $C=0.52$ ,  $\varepsilon=0.03$ .

$$T^{-1/2} \left( \int_0^T [X_1^2(t) + Y_1^2(t) + X_2^2(t) + Y_2^2(t)] dt \right)^{1/2},$$

where  $T$  is a period. The antiphase mode loses stability as coupling is increased but its period increases only slightly, even if the mode overlaps with the stable inhomogeneous steady states.

The system of coupled oscillators (1) was solved by direct integration under more intensive coupling in order to find new regimes onto which the system settles after the pitchfork bifurcation. We discovered a set of solutions which are characterized by the presence of the different numbers of loops on the phase portrait. Figures 7(a,b) present an example of waveforms and the phase portrait of the limit cycle with six

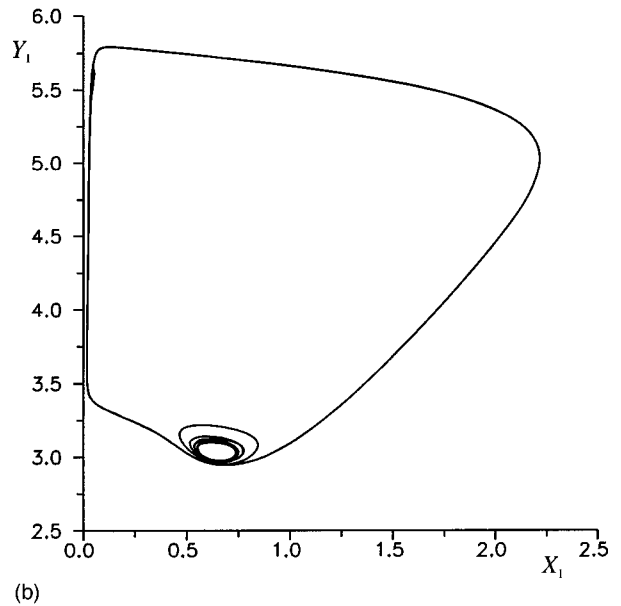


FIG. 7. The wave form (a) and phase portrait (b) of the antiphase mixed-mode regime at  $\eta=2.56$ ,  $C=0.55$ .

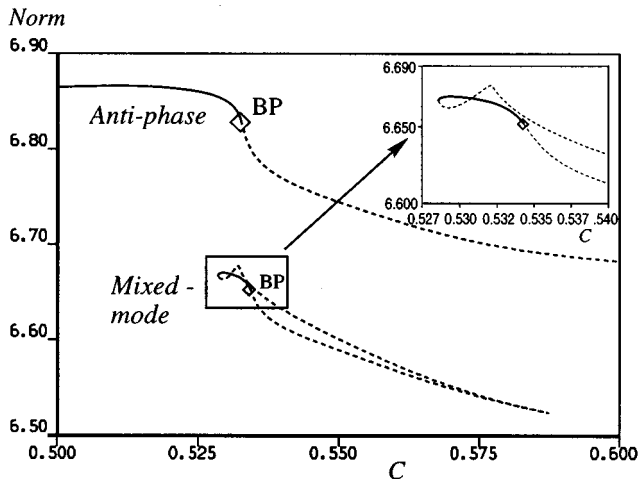


FIG. 6. Continuation of antiphase and one-looped mixed-mode solutions for  $\eta=2.56$ ,  $\varepsilon=0.03$ . Solid curves denote asymptotically stable solutions, and dashed curves denote unstable solutions.

loops. It is easy to see that the large parts of the trajectories consist of the high-frequency low-amplitude oscillations. The full period of the mixed-mode cycle is typically significantly greater than that of the antiphase mode. The wave forms the mixed-mode cycles are invariant with respect to the  $T/2$  time shift. Therefore, we will call these solutions “antiphase mixed modes.” This four-dimensional limit cycle has coincidental projections in the  $(X_i, Y_i)$  planes of each oscillator.

The area in the parameter plane that contains antiphase mixed-mode cycles is enlarged in Fig. 8 to clarify the details. The dotted line is the boundary of the stable inhomogeneous stationary solutions. The set of stripes marks the areas cor-

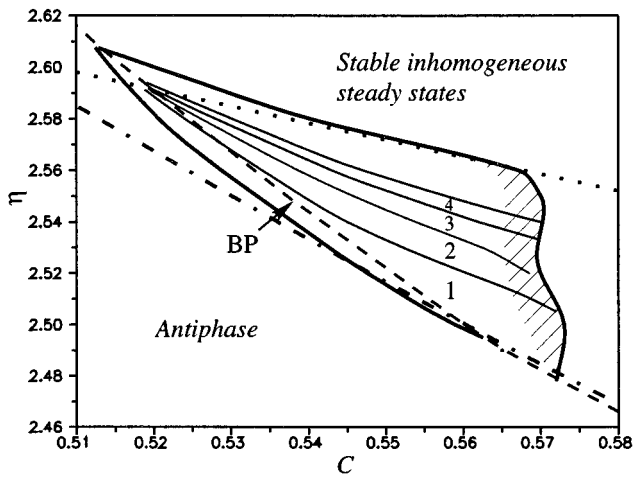


FIG. 8. The small scale phase diagram for mixed-mode solutions for  $\varepsilon=0.03$ . The numbers mark the regions with  $n$ -looped cycles. The thick solid line outlines the region of all kinds of mixed-mode regimes. Other designations are indicated in the text.

responding to antiphase mixed-mode limit cycles with different numbers of loops. One can see in Fig. 8 that the stable antiphase mixed-mode and simple antiphase regimes can coexist (the dashed line is a continuation of BP along the branch of the antiphase solution). It is essential to note that the more stiff the isolated oscillator is, the larger the area that is occupied by the mixed-mode (regardless of the number of loops), and the smaller the sizes of the loops.

The appearance of antiphase mixed-mode cycles may be considered a result of the interaction between the antiphase mode and a spatially inhomogeneous limit cycle (ILC) that emanates via the Hopf bifurcation (see [18]) of the stable inhomogeneous steady state. The ILC locates around an unstable focus that is an inhomogeneous stationary solution outside the region of stable inhomogeneous steady states. This four-dimensional limit cycle has noncoincident projections in the  $(X_i, Y_i)$  planes of each oscillator (see Fig. 9). The frequency of small oscillations in the mixed mode corresponds to the frequency associated with the unstable focus and the ILC. The ILC's are "separatrix" cycles that characterize the part of the phase flow oscillating around the focus.

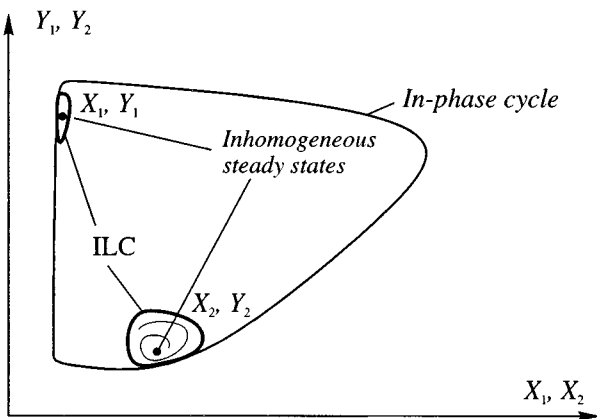


FIG. 9. The projection of phase portrait of the inhomogeneous limit cycle (ILC) in comparison with one of the in-phase cycle.

When parameters are chosen near the area of stable inhomogeneous states, a part of the antiphase cycle passes close to the unstable focus. If coupling is great enough, the representative point is captured by the rotating field of the focus. This part of the cycle is then replaced by a helical trajectory with one or more winds. AUTO shows that the substitution is not a bifurcation to the torus or period doubling. The one-parameter continuation of the one-looped mixed-mode cycle (Fig. 6) discovers that this regime manifests as a closed curve without any evidence of bifurcations to other attractors. Such solutions are typically referred to as "isolas." One-, two- and  $n$ -looped mixed-mode regimes appear as isolated solutions and coexist with the neighbors.

Inside the stripes of the multilooped mixed-mode regimes, the phase flux around the inhomogeneous focus is very complex, because the ILC's undergo the period doubling bifurcation sequence. The set of ILC families with numerous local maxima was studied in [22], but for very strong coupling ( $C \sim 10$ ) of two Brusselators taken near the Hopf bifurcation. It was shown that the infinity of periodic solutions and chaotic attractors exist. Using the package AUTO we found that for the coupled membrane oscillators all the ILC's are always unstable and are located inside the strip along the boundary of the inhomogeneous steady states. Their amplitudes and frequencies correspond to those of the small oscillations in the antiphase mixed mode. That is why the boundary of the parameter set at which the ILC exists (dashed and dotted lines in Fig. 8) outlines the region on parameter plane where the system of oscillators (1) has mixed-mode cycles.

Any antiphase limit cycles found for the model of coupled membrane oscillators can be bistable with the inhomogeneous steady states (although the areas of overlapping are very small). The penetration of the mixed-mode regime into the inhomogeneous steady-state area is a specific feature of the model (1). The period of the mixed-mode regime depends on the number of loops; the function  $T(C)$  demonstrates infinite period bifurcation in the area of overlap with the inhomogeneous steady states (Fig. 10), whereas AUTO continuation of the simple antiphase solution in two parameters shows that this stable periodic solution has the *finite* period everywhere along the boundary of its extinction.

The phase diagram for two coupled Brusselators taken far from the Hopf bifurcation of their birth is almost the same as that for membrane oscillators, but there is the parameter set where the ILC's are stable [18,22]. The regions corresponding to the anti-phase mixed-mode regimes, the ILC, and stable inhomogeneous steady states are shown in Fig. 11. The strip of the one-looped mixed-mode cycle is drawn (denoted by 1), but other strips of the 2-, and 3- looped cycles are too narrow to be pictured on this scale. When  $C$  is increased but  $B$  is fixed the period of the mixed-mode regime grows but does not tend to infinity because inhomogeneous steady states are unstable. Moreover, penetration of the mixed-mode regime into the area of the stable inhomogeneous steady states is impossible: the stable ILC separates them from the inhomogeneous steady states. We believe that the antiphase mixed-mode regimes are distinct from the one-looped solution observed by Shreiber *et al.* (Fig. 11 in [22]) because the latter solution undergoes an infinite period bifurcation due to the lengthening of the flat part of the trajectory. Its loop is not linked with the rotation around the inhomoge-

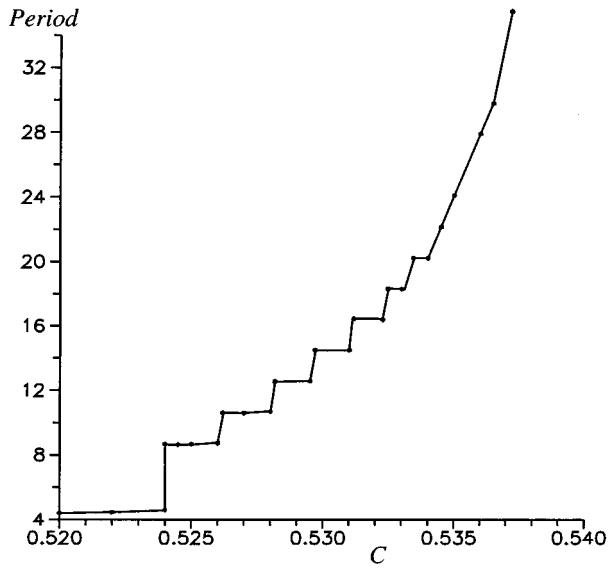


FIG. 10. Period of antiphase mixed-mode cycles vs the coupling  $C$  at  $\eta=2.58$ ,  $\varepsilon=0.03$ .

neous steady state so the loop appears under smaller values of coupling than these steady state.

**C. Symmetry breaking bifurcation**

Each of the antiphase mixed-mode solutions of (1) bifurcates via the symmetry breaking bifurcation BP (open square in Fig. 6) to the secondary branch containing stable unsymmetrical solutions. Figure 12 shows the regime where the first oscillator has no loop at the lower part of the wave form while the second one has one loop demonstrating breaking of the spatiotemporal symmetry. Such attractors emerge typically as the boundaries between the antiphase mixed-mode regimes with  $N$  and  $N + 1$  number of loops (although it is not obligatory). The parametrical continuation made by AUTO

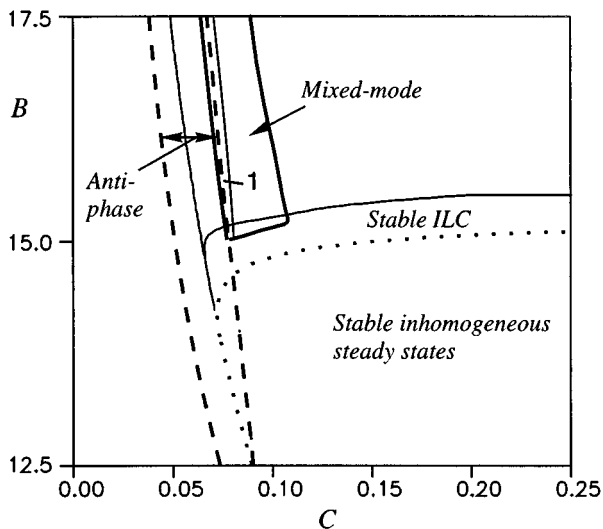


FIG. 11. The phase diagram for two coupled Brusselators at  $A=2$ . The thick solid line outlines the region of all kinds of mixed-mode regimes.

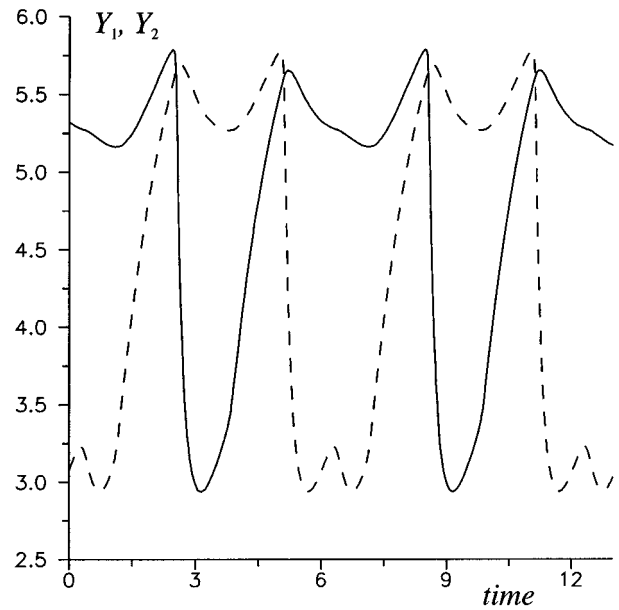


FIG. 12. The wave form of the out-of-phase mixed-mode cycle for (1) at  $\eta=2.485$ ,  $C=0.57$ ,  $\varepsilon=0.03$ .

shows that the branch of the out-of-phase mixed-mode solutions is an isola (see Fig. 13). The unsymmetrical solutions produce a tertiary periodic branch via the period doubling bifurcation and so on. We found here a cascade of period doubling bifurcations and, therefore, there is an infinite structure of stable periodic and nonperiodic solutions in the region of parameters. The cross-hatched area in Fig. 8 shows the parameter set where quasiperiodic and chaotic regimes have large basins of attraction.

**V. DISCUSSION**

It is well known that the coupling of even identical oscillators can result in the appearance of a variety of attractors, including the stable inhomogeneous steady states. The antiphase regime was found in many systems and was proved

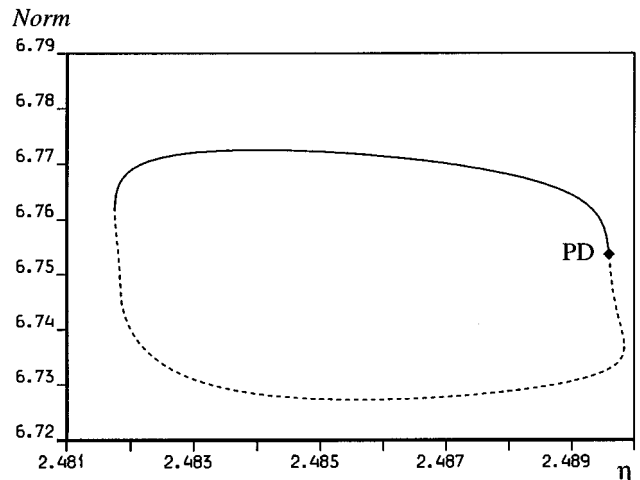


FIG. 13. Bifurcation diagram of the out-of-phase mixed-mode cycle. Period doubling bifurcations are denoted by PD.

analytically for the case of weak coupling [16,15]. It has been shown already that the antiphase regime that exists in the system of relaxation oscillators under strong coupling has the peculiarities that might be essential for the interpretation of biological and chemical experiments [6,18].

The mixed-mode regime should be outlined, first, as a periodic solution that possesses the second time scale in addition to the period of the antiphase solution. For very stiff oscillators these high-frequency oscillations are practically unobservable and the coupling changes only the amount of time spent by the system on different parts of the trajectory. Under the intermediate stiffness, the presence of the second time scale should be taken into account if the influence of external oscillator would be considered, for example.

Second, an analysis of the full phase diagram shows that there is such a region of the control parameters where the mixed-mode regime transits to the inhomogeneous steady states via infinite period bifurcation (see Fig. 10). Besides, the antiphase mixed-mode cycles can coexist with the antiphase regime and the stable inhomogeneous steady states, providing a hysteresis between these attractors.

Another interesting regime is the inhomogeneous limit cycle. Generally speaking, the ILC should be considered as a typical oscillatory pattern because one type of the ILC emerges from the inhomogeneous steady state via the Hopf bifurcation, e.g., if the coupling strength decreased. For the

oscillators with the  $N$ -shaped nullcline, the amplitude of the stable ILC is so small that the ILC is practically indistinguishable in the steady state (except for the oscillatory external signal of appropriate frequency).

The model (1) demonstrates the out-of-phase mixed-mode cycles (see Fig. 12 as an example). These cycles are observable for the intermediate stiffness only ( $0.01 < \varepsilon < 0.06$ ). Despite the small areas occupied by these solutions in a parameter plane, they seem to be of principle importance because their existence may be considered as the phenomenon "broken spatio-temporal symmetry" but for the limit cycles.

A comparison of coupled membrane oscillators (1) with coupled Brusselators shows that the properties examined are general and are realized if the stiffness is greater than a certain critical value. The observability of these peculiarities is quite problematical due to the small areas of hysteresis on the phase diagram and small amplitude of loops in the mixed-mode regime. But if the experimental system has the parameters that robustly control the stiffness and the position of oscillators with respect to the bifurcation of their birth, then the obtained regimes and transitions may be observed.

#### ACKNOWLEDGMENT

The authors gratefully acknowledge Professor H.B. Keller for the use of the package AUTO.

- 
- [1] J. P. Gollub, T. O. Brunner, and B. G. Danly, *Science* **200**, 48 (1978).
- [2] J. Berkemeier, T. Dirksmeyer, G. Klempt, and H.-G. Purwins, *Z. Phys. B* **65**, 255, (1986).
- [3] D. A. Linkens, I. Taylor, and H. L. Duthie, *IEEE Trans. Biomed. Eng.* **23**, 101 (1976).
- [4] I. R. Epstein, *Commun. Mol. Cell. Biophys.* **6**, 299, (1990).
- [5] K. J. Bar-Eli, *J. Phys. Chem.* **88**, 3616, (1984).
- [6] M. F. Crowley and I. R. Epstein, *J. Phys. Chem.* **93**, 2496, (1989).
- [7] B. Lavenda, G. Nicolis, and M. Herschkowitz-Kaufman, *J. Theor. Biol.* **32**, 283 (1971).
- [8] J. Gerhart, M. Wu, and M. Kirschner, *J. Cell. Biol.* **98**, 1247 (1986).
- [9] M. J. Berridge and P. E. Rapp, *J. Exp. Biol.* **81**, 217 (1979).
- [10] G. Gerisch and V. Wick, *Biochem. Biophys. Res. Commun.* **65**, 364 (1975).
- [11] R. Lefever, and I. Prigogin, *J. Chem. Phys.* **48**, 1695 (1968).
- [12] K. Bar-Eli, *J. Chem. Phys.* **94**, 2368 (1990).
- [13] A. T. Mustafin and E. I. Volkov, *Biol. Cybern.* **49**, 149 (1984).
- [14] J. J. Collins and I. M. Stewart, *J. Nonlin. Sci.* **3**, 349 (1993).
- [15] P. J. Holmes and R. H. Rand, *Int. J. Non-Linear Mech.* **15**, 387 (1980).
- [16] H. G. Othmer, D. G. Aronson, and E. J. Doedel, *Physica D* **25**, 20 (1987).
- [17] D. G. Aronson, G. B. Ermentrout, and N. Kopell, *Physica D* **41**, 403 (1990).
- [18] E. I. Volkov and V. A. Romanov, *Phys. Scr.* **51**, 19 (1995).
- [19] D. Ruwich, M. Bode, P. Schutz, and M. Markus, *Phys. Lett. A* **186**, 137 (1994).
- [20] I. Stuchl and M. Marek, *J. Chem. Phys.* **77**, 1607 (1982).
- [21] M. N. Stolyarov and E. I. Volkov, *Phys. Lett. A* **159**, 61 (1991).
- [22] I. Shreiber, M. Holodniok, M. Kubíček, and M. Marek, *J. Stat. Phys.* **43**, 489 (1986).
- [23] V. Petrov, S. K. Scott, and K. Showalter, *J. Chem. Phys.* **97**, 6191 (1992).
- [24] J. Honerkamp, G. Mutschler, and R. Seitz, *Bull. Math. Biol.* **47**, 1 (1985).
- [25] D. S. Chernavskii *et al.*, *BioSystems* **9**, 187 (1977).
- [26] E. J. Doedel, N. G. Keller, and J. P. Kernevez, *Int. J. Bifurcation Chaos* **1(3)**, 493 (1991); **1(4)**, 745 (1991).
- [27] J. M. T. Thompson, H. B. Stewart, and Y. Ueda, *Phys. Rev. E* **49**, 1019 (1994).